34th Annual International Conference of the IEEE EMBS
San Diego, California USA, 28 August - 1 September, 2012

Cortical bone quality assessment using quantitative ultrasound on long bones

Josquin Foiret, Jean-Gabriel Minonzio, Maryline Talmant, and Pascal Laugier

Abstract — **The potential of ultrasonic guided waves to identify geometrical and elastic properties of long cortical bone was tested in this feasibility study. In this paper, we present the general framework of the inversion process applied to guided waves measurements performed on test cases and on one in vitro sample of human long cortical bone (forearm). Test cases were flat plates of bone mimicking material. Cortical thickness and direction dependent elastic properties of a long cortical bone were identified from ultrasound guided waves measurements. While the results need to be confirmed on a large set of bone specimens, this study opens new perspectives for axial transmission technique, due to the fact that measurements were performed under actual conditions of clinical measurements, *i.e.* with a probe and a signal processing dedicated to clinical use.**

Index Terms— **axial transmission; guided wave; cortical bone; quantitative ultrasound; singular value decomposition .**

I. Introduction

Quantitative ultrasound (QUS) techniques have been developed in the past two decades to assess bone status and fracture risk. The significant growth of the QUS research field has been based on the affordability of this non-ionizing technology and the potential of ultrasound waves to probe bone quality features, beyond the bone mineral density which is currently assessed using X-ray densitometry. Recent studies pointing towards the importance of cortical bone motivates one important aspect of the research presented in the present study which is to focus measurements on cortical bone. About 80% of fractures, occurring after age of 60 years when the rate of cortical bone loss overpasses that of trabecular bone [1], arise at cortical sites. In addition, the cortical shell contributes 40-90% of the bending rigidity [2] and cortical porosity is a crucial factor determining the bone fragility that underlies non vertebral fracture risk in women older than 65 years [1]. The recent results mentioned above suggest that diagnosis (risk assessment) should include accurate evaluation of cortical bone to improve identification of individuals at high and low risk of fracture.

QUS technologies were adapted for long cortical bone [3]. The configuration, referred to as the axial transmission technique (ATT) is based on ultrasound propagation along the bone axis. Prediction of fracture risk with ATT and X-ray densitometry was found to be similar in pilot studies [4]. In these studies, the analysis of ultrasound signals from ATT was reduced to a unique ultrasound parameter: the velocity of the first arriving signal obtained from time of flight measurements [5]. The paradigm of ATT moved recently to the determination of risk factors, such as cortical thickness [6] and elastic properties [7] based on inversion of ultrasound measurements. The key point which allowed this progress was (i) considering cortical bone as a waveguide sustaining the propagation of guided waves and development of appropriate models of propagation in cortical bone and (ii) the introduction of signal processing tools which provided multiple ultrasound parameters, used as input in inversion procedures to identify model parameters. The large set of ultrasound parameters used for the inversion consists in the characteristics of guided waves which propagate in bones, let us say a set of pairs (frequencies, wavenumbers), (f_{exp},k_{exp}) related to these guided waves. These approaches are inspired by the methodology adopted in other research fields such as non destructive testing to identify properties of waveguides [8,9]. However, several adaptation of known methods were required to address the dedication of these tools to clinical measurements of long bones. For instance, a compact linear array of sources and receivers is used for clinical examination in place of a single moving receiver. The limited access to cortical bone site, limiting the length of the receiving array and preventing the use of classical tools such as two-dimensional Fourier transform to convert the data from (time-space) plane to (frequency-wavenumber) plane, is overcome with a dedicated signal processing technique which is summarized thereafter. The inversion scheme is adapted for the combined determination of cortical thickness and stiffnesses, whereas in other research fields inversion schemes focus mostly on the determination of stiffnesses and mass density, the geometrical parameter being known. Finally, a dedicated measurement protocol need to be developed, due to the irregular geometry of bone and to the increased degree of freedom related to the presence of soft tissue.

In this paper, all experiments are achieved on the forearm (radius) using an array of transmitters/receivers designed for clinical use. The raw ultrasound data consist of a series of signals obtained for all pairs of emitter-receiver. The time series are then processed with an approach based on the singular value decomposition (SVD) of multidimensional signals as introduced in [10]. From the set of experimentally measured (frequency, wavenumbers) (f_{exp}, k_{exp}), both elastic and geometrical properties of a sample of human cortical bone were reconstructed, using the model of Lamb waves in a transverse isotropic flat plate. The inversion process was first validated with experiments performed with the same device and signal processing on bone mimicking flat plates.

Authors are with CNRS - UPMC Univ Paris 6 - UMR 7623, 15 rue de l'école de médecine, 75006 Paris, France

II. Signal Processing

A 1 MHz broadband linear array (Vermon, Tours, France) was used. For the sake of completeness, the main lines of the SVD-based signal processing technique are recalled [11,12]. The recorded signals $r_{ij}(t)$, with i and j the emission and reception indices ranging from 1 to N^E and 1 to N^R, respectively, are first Fourier-transformed, resulting in a $N^E \times N^R$ matrix R with element $R_{ij}(f)$ for each frequency f. In this paper, $N^E = 5$, $N^R = 32$. At each frequency f, the R matrix is decomposed according to its singular values and vectors. Signal to noise separation is then achieved by applying a first heuristically selected threshold t_1 on the singular values. The basis of the signal subspace is then constituted of the M reception singular vectors, denoted $\mathbf{U}_m$, such that their associated singular values are higher than t_1. Normalized spatial plane waves defined on the reception array are subsequently decomposed on the basis $\mathbf{U}_m$, giving rise to the so-called *Norm* function defined by:

$$Norm(f,k,\alpha) = \sum_{m=1}^{M} \left| \left\langle \mathbf{U}_m \left| \mathbf{e}^{test}(k,\alpha) \right\rangle \right|^2, \qquad (1)$$

where $\boldsymbol{e}^{test}(k,a)$ is proportional to $exp(i(k + ia)x^R)$ with k and α the real and imaginary parts of the testing wavenumber.

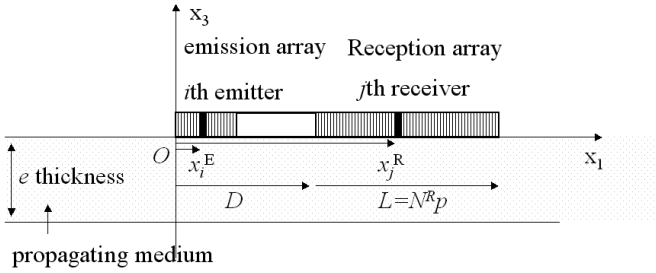

Fig.1. AT configuration with multi-emitters and multi-receivers arrays.

The scalar product $< \boldsymbol{U}_n \mid \boldsymbol{e}^{test}(k,a) >$ corresponds to the normalized spatial Fourier transform of the singular vector $\mathbf{U}_n$. Thus, the SVD can be interpreted as a denoising step between the temporal and spatial Fourier transforms. Maxima in the *Norm* function, scaled from 0 to 1 by definition, provide the pairs (f_{exp}, k_{exp}) of the guided waves efficiently excited in the waveguide. The SVD approach is more efficient than two dimensional Fourier transform particularly for small receiving array and dissipative materials [10].

III. Samples

For validation purpose, four 1.25, 2.25, 3.35 and 4.15 mm-thick bone-mimicking plates (short glass fibers embedded in an epoxy matrix, Sawbones®, Pacific Research, Vashon, WA USA) were investigated. Values of compressive and tensile moduli of the plates (transverse isotropic) are close to those of human cortical bone. For comparison, ultrasound-based identification of model parameters are compared to reference values. Bulk wave velocities were measured in the laboratory by through transmission measurements with contact transducers on a 10mm-thick plate of the same material [11]. Plate thickness was measured with a calliper. For feasibility test on in vitro experiments, one sample of human radius was also examined.

IV. Model Parameters Identification

The general framework of an inversion process is to choose a model in which measured quantities vary with some parameters (model parameters). By minimizing the deviation between experiments and model predictions, parameters of the experiments are identified to values of the model parameters. A cost function is build to evaluate the minimal shift reached through the application of an optimization algorithm, here a non-linear least-square process.

In this work, the model used is the propagation of Lamb waves in an infinite flat plate made of homogeneous transverse isotropic material. Lamb waves are described by a dispersion equation $F_{A,S} = 0$, for pairs of (frequencies, wavenumbers) (f, k) which vary with the plate thickness and with its elastic properties. Fig. 2 shows the dispersion function F_A for fixed values of material properties in the plane (fe, ke). Dispersion curves of each branch display as narrow zeroes.

The cost function used in the least square algorithm χ involves the value of the dispersion function $F_{A,S}$ as

$$\chi = \sum_{j=1}^{J} \sum_{i=1}^{I_j} \left| F_{A,S}\left(k_{i,\exp}, f_{i,\exp} \;;\; P\right) \right|^2 . \qquad (2)$$

with subscripts A and S referring to the symmetry of the particle motion involved in a specified branch (respectively anti-symmetric and symmetric) and P is the set of model parameters as defined below. The sum with the subscript j refers to the number of experimentally determined portion of dispersion curves and the subscript i refers to the number of experimentally measured pairs of frequency-wavenumber ($f_{i,exp}$, $k_{i,exp}$). The experimentally determined pairs ($f_{i,exp}$, $k_{i,exp}$) are supposed to be Lamb branches and therefore all satisfy $F_A = 0$ or $F_S = 0$, thus make the cost function null for a set of model parameters, called P in (2). The set of model parameters P can be defined in several ways, as long as P includes the thickness e (or here the ratio thickness over velocity), in addition to the absolute value of at least one velocity and in addition to three anisotropy ratios. In this paper P was chosen as:

$$P = \{V_T, e/V_T, c_{13}/c_{33}, c_{11}/c_{33}, c_{33}/c_{55}\} .$$

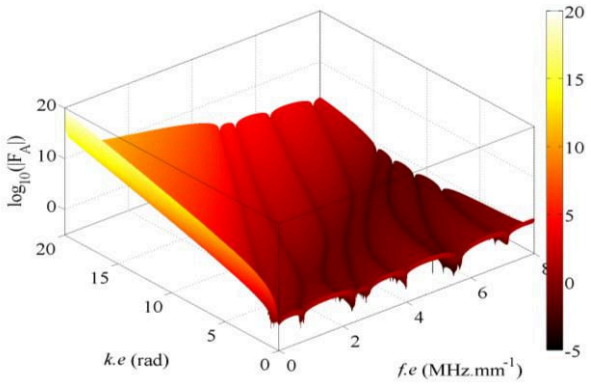

Fig. 2. Dispersion function for the antisymmetric Lamb modes as function of frequency×thickness and wavenumber×thickness for a fixed set of model parameters P.

As indicated in Fig. 1, axis x1 refers to the direction of fibers, x3 refers to the direction normal to the fibers, V_T is the bulk shear wave velocity propagating in the direction of the fibers (or propagating across fibers with a polarization parallel to fibers, assuming transverse isotropic symmetry) $V_T = [c_{55}/\rho]^{1/2}$, and c_{ij} refers to the stiffness according to the definition of the axis. Note that in this formulation, *a priori* knowledge of mass density is not requested.

V. Pre-processing

Pre-processing of the experimental data aims in reconstructing branches of dispersion curves. Maxima of the Norm function ($f_{i,exp}$, $k_{i,exp}$) are first classified into a set of branches, each of one assumed to be a part of a dispersion curve. This step is achieved by semi automatically taking into account the continuous behavior of k_{exp} as function of f_{exp}. Let us remark that it is not required to *a priori* allocate the label A_0, S_0, ... [12,13] to these experimentally determined portion of dispersion curves. Finding the symmetry properties (A or S) is a part of the identification procedure. A symmetry is arbitrarily assign to each experimentally defined branch and then the minimization is applied to 2^J combinations of symmetries for the set of J sections of branches. Alternatively, a quick answer for the best symmetry is the calculation of the cost function for the 2^J combinations of symmetries, for arbitrary set of anisotropy ratios. Inversion process is then achieved for selected combinations of symmetries, which gives the minimum values of the cost function.

VI. Results

All the specimens considered here were measured with the probe aligned parallel to the fibers. One example of experimental measurements are shown on Fig. 3 for the thinnest plate, (e = 1.25mm). A quick observation shows that experimentally determined branches does not exhibit as continuous and complete branches as calculated branches do. It is expected due to the unavoidable limited sensitivity of the probe combined to the frequency dependent excitation efficiency of each branch. In our configuration, this phenomenon is related mostly to the frequency dependence of the normal component of the particle displacement involved specifically in each branch. The discontinuous and incomplete character of experimentally determined spectrum orientated the choice of the cost function we have made, using the dispersion function and not the solution (f, k) of the dispersion function, which are directly comparable to experimental data but requires to have identified first the related branch. For that plate, operator have chosen J = 5 branches, according to the apparent continuity of the curves.

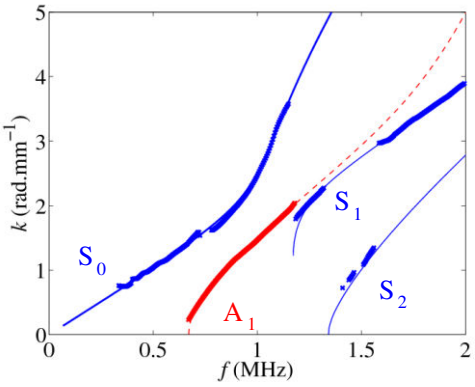

Fig. 3. Experimental wavenumber (×) as function of frequency for the 1.25 mm bone mimicking plate. The theoretical plate model calculated using the estimated parameters is plotted with the continuous and dashed lines (respectively symmetric and anti-symmetric modes).

Thickness and elastic properties of the 4 plates estimated by the inversion process are compared to reference values in Fig. 4 and 5. For comparison purpose, anisotropy ratios were expressed as bulk wave velocities which are available from the reference contact transmission measurements. Reference thickness of the plates are obtained with a caliper. An overall agreement is observed, despite a slight underestimation systematically observed on thickness and noticeable variability of the estimated bulk velocities. Although the material was considered to be identical for all the phantoms, we cannot exclude that slight variations in their composition may contribute partly to the measured variability. In addition, as plates of different thickness were measured, the number of experimental modes for each of them was different and this impacts the accuracy of the estimation.

The experimental spectrum of guided waves measured on the human radius sample is shown in Fig.6. Note the similarities with the spectrum obtained on the 1.25 mm-thick bone mimicking plate. Inversion procedure provided a thickness of 1.62 ± 0.05mm and values of bulk wave velocities of 4110±110m.s^{-1} and 3060±180m.s^{-1} for the compression waves propagating along and across the fibers, respectively, and 1780±70m.s^{-1} for the shear wave. The estimated cortical thickness (1.62mm) is consistent with that measured on the contra-lateral radius (1.5 mm) of the same subject with microcomputed tomography. Independent estimates of the compression and shear velocities were not available for the investigated specimen. However, note that estimated values fall in the range of values commonly reported for cortical bone at this frequency.

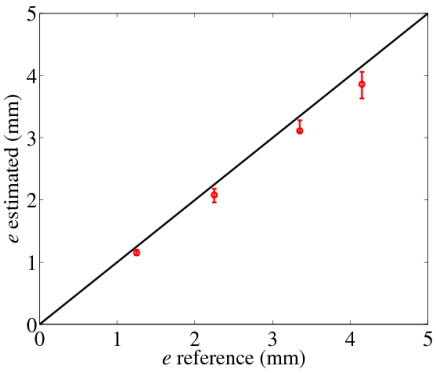

Fig. 4. Estimated thickness compared to the reference value (caliper). The error bars indicate the range between maximum and minimum value.

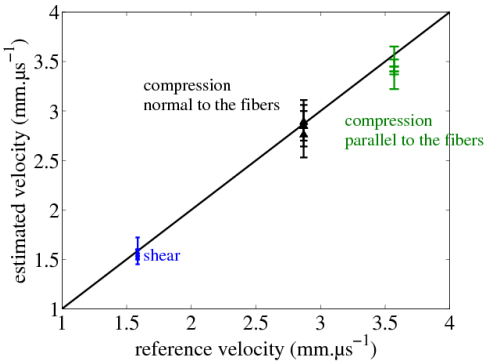

Fig. 5. Estimated bulk wave velocities compared to reference values. The error bar indicate the range between maximum and minimum value.

VII. Conclusion

This study represents a significant step toward the characterization of bone properties from ultrasound measurements. We have shown that our experimental data, while impaired by several mechanisms such as absorption in bone, allow to evaluate cortical thickness and elastic properties. Estimated stiffnesses on test cases (bone-mimicking flat plates) display some variability, likely due partly to the different amount of information available in the experiments in thin and thick plates. However, the study shows that the inversion process should allow discrimination between plates of different thickness. Further study will address the robustness of in vitro determination of bone properties in a large set of specimens as well as extension of the method to *in vivo* measurements.

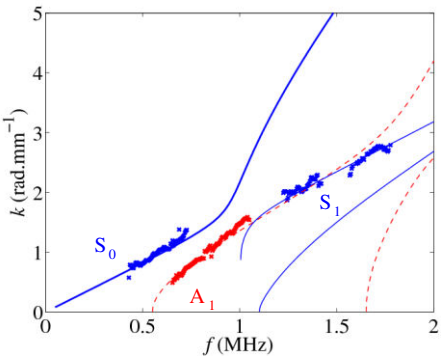

Fig. 6. Experimental wavenumber (×) in function of the frequency for a human radius. The plate modes calculated using the estimated parameters is plotted with the continuous (symmetric) and dashed lines (anti-symmetric).

References

[1] R.M.D. Zebaze, A. Ghasem-Zadeh, A. Bohte, S. Iuliano-Burns, M. Mirams et al., "Intracortical remodelling and porosity in the distal radius and post-mortem femurs of women: a cross-sectional study", *Lancet,,* vol. 375, pp: 1729-36, 2010.

[2] G. Holzer, G. Von Skrbensky, L.A. Holzer, and W. Pichl, "Hip fractures and the contribution of cortical versus trabecular bone to femoral neck strength", J Bone Miner Res, vol 24, pp. 468-74, 2009

[3] P. Moilanen, "Ultrasonic guided waves in bone", IEEE Trans Ultrason Ferroelec Freq Contr, Vol 55, pp.1277-86, 2008

[4] D. Hans, L. Genton, S. Allaoua, C. Pichard, and D. O. Slosman, "Hip fracture discrimination study - QUS of the radius and the calcaneum," *J Clin Densitom*, vol. 6, pp. 163-72, 2003.

[5] E. Bossy, M. Talmant, M. Defontaine, F. Patat, and P. Laugier, "Bidirectional axial transmission can improve accuracy and precision of ultrasonic velocity measurement in cortical bone: A validation on test materials," *IEEE Transs Ultrasonics Ferroelecs Freq Contr*, vol. 51, pp. 71-9, 2004.

[6] P. Moilanen, P.H.F. Nicholson, V. Kilappa, S. L. Cheng, and J. Timonen, "Assessment of the cortical bone thickness using ultrasonic guided waves: Modelling and in vitro study," *Ultrasound Med Biol*, vol. 33, pp. 254-62, 2007.

[7] F. Lefebvre, Y. Deblock, P. Campistron, D. Ahite, and J. J. Fabre, "Development of a new ultrasonic technique for bone and biomaterials in vitro characterization," *J Biomed MaterRes*, vol. 63, pp. 441-6, 2002.

[8] M.R. Karim, A.K. Mal, and Y. Barcohen, "Inversion of Leaky Lamb Wave Data by Simplex Algorithm," *J Acoust Soc Am*, vol. 88, pp. 482-91, 1990.

[9] W. P. Rogers, "Elastic Property Measurement Using Rayleigh-Lamb Waves," *Res Nondestruct Eval*, vol. 6, pp. 185-208, 1995.

[10] J.G. Minonzio, M. Talmant, and P. Laugier, "Guided wave phase velocity measurement using multi-emitter and multi-receiver arrays in the axial transmission configuration," *J Acoust Soc Am*, vol. 127, pp. 2913-9, 2010.

[11] J.G. Minonzio, J. Foiret, M. Talmant, and P. Laugier, "Impact of attenuation on guided mode wavenumber measurement in axial transmission on bone mimicking plates " *J. Acoust. Soc. Am.*, vol. 130, pp. 3574-82, 2011.

[12] J.L. Dean, C. Trillo, A.F. Doval, and J. L. Fernandez, "Determination of thickness and elastic constants of aluminum plates from full-field wavelength measurements of single-mode narrowband Lamb waves," *J Acoust Soc Am*, vol. 124, pp. 1477-89, 2008.

[13] C.-H. Yeh and C.-H. Yang, "Characterization of mechanical and geometrical properties of a tube with axial and circumferential guided waves," *Ultrasonics*, vol. 51, pp. 472-9, 2011.